



Original research

Optimization and development of insulin nanoparticles by new thiolated chitosan derivative with ionic gelation method using a model-based methodology

Zahra Mahdizadeh Barzoki^{a,b}, Zahra Emam-Djomeh^{a,c,*}, Morteza Rafiee-Tehrani^d, Elaheh Mortazavian^d, Ali Akbar Moosavi Movahedi^e

^a Transfer Phenomena Laboratory (TPL), Department of Food Science, Technology and Engineering, Faculty of Agricultural Engineering and Technology, College of Agriculture and Natural Resources, University of Tehran, PO Box: 4111, 31587-11167 Karaj, Iran

^b Faculty of food industry and agriculture, Standard Research Institute (SRI), Karaj, Iran

^c Center of Excellence for Application of Modern Technologies for Producing Functional Foods and Drinks

^d Department of Pharmaceutics, Faculty of Pharmacy, Tehran University of Medical Sciences, Tehran, Iran

^e Institute of Biochemistry & Biophysics (IBB), University of Tehran, Tehran, Iran

ABSTRACT

Insulin therapy has been the best choice for the clinical management of diabetes mellitus. The current insulin therapy is via subcutaneous injection, which often fails to mimic the glucose homeostasis that occurs in normal individuals. Oral delivery is the most convenient administration route. However, insulin cannot be well absorbed orally because of its rapid enzymatic degradation in the gastrointestinal tract. Therefore, nanoparticulate carriers such as polymeric nanoparticles are employed for the oral delivery of insulin. This study aims at the statistical optimization by Box-Behnken statistical design, fabrication by ionic gelation technique and in vitro characterization of insulin nanoparticles containing thiolated N-dimethyl ethyl chitosan (DMEC-Cys) conjugate. Independent variables such as the concentrations of polymer, TPP and insulin were optimized using a 3-factor, 3-level Box-Behnken statistical design. The selected dependent variables were size, zeta potential, PdI and associated efficiency of nanoparticles. The optimized nanoparticles were shown to have mean particle size diameter of 148 nm, zeta potential of 15.5 mV, PdI of 0.26 and AE of 97.56%. In vitro release study, FTIR, FE-SEM and cytotoxicity also indicated that nanoparticles made of this thiolated polymer are good candidate for oral insulin delivery.

Keywords: Drug Carrier, Oral drug delivery, Optimization, Nanoparticles

Received 14 December 2017; Received 1 April 2018; Accepted 10 April 2018

1. Introduction

Diabetes is one of the most common metabolic disorders that threatens community health and also one of the most principle causes of mortality and morbidity (Jamshidi, 2012). Due to its high prevalence and secondary effects, diabetes is one of the most lethal diseases and responsible for almost three million deaths per year worldwide, as reported by the World Health Organization. On average, life expectancy is reduced by more than 20 years in people with type 1 diabetes and by up to 10 years in people with type 2 diabetes (Khafagy et al., 2007). The subcutaneous route has been the mainstay of insulin delivery until now. The burden of daily injection, physiological stress, pain, inconvenience, cost, risks, infection, inability to handle insulin and localized insulin deposition leading to local hypertrophy and fat deposition at the

injection sites still remain as problems (Khafagy et al., 2007). Despite significant advancement in the field of pharmaceutical research, development of a proper and non invasive insulin-delivery system remains a major challenge (Avadi et al., 2010). Micro and nanosphere encapsulation is the only drug delivery vehicle that has the potential to surpass both enzymatic and physical barriers of the GI tract in therapeutic proteins such as insulin (Morishita et al., 2006; Couvreur, 2013).

Various methods have been used for preparation of insulin nanoparticles composed of chitosan derivatives. Among different techniques for synthesizing nanoparticles, ionic gelation with tripolyphosphate (TPP) as the cross linker is the mostly adopted technique to fabricate chitosan nanoparticles; since this method is simple, mild, less toxic and suitable for scaling up (Dong et al., 2013; Fan et al., 2012; Hu et al., 2008). Cationic nature of chitosan shows good mucoadhesive and membrane permeability properties.

*Corresponding author.

E-mail address: emamj@ut.ac.ir (Z. Emam-Djomeh).

The mechanisms of mucoadhesive and membrane permeation is based on interaction of positive charges with negatively charged cell membrane and prevent structural recognition by membrane associated gate proteins, respectively. Calvo et al. (1997) developed ionic gelation method for preparing hydrophilic polymers such as chitosan. The size of nanoparticles is affected by chitosan and TPP concentrations. To prevent flocculation, nanoparticle concentration must be kept at low level (Fan et al., 2012; Vaezifar et al., 2013; Mohammadpourounighi, 2010). In this method, positively charged amino group of chitosan interacts with negative charged TPP to form coacervates with a size in the range of nanometer. Coacervates are formed as a result of electrostatic interaction between two aqueous phases (Mohammadpourounighi et al., 2010; Nagavarma et al., 2012; Li et al., 2008; Vimal et al., 2013). Dustgania, et al. (2008) prepared dexamethasone sodium phosphate-loaded chitosan nanoparticles by ionic gelation method. Mortazavian, et al. (2014) synthesized two new generations of thiolated N-diethyl methyl chitosan and N-dimethyl ethyl chitosan, and prepared insulin nanoparticle of 174 nm with dimethylethyl chitosan cysteine (DMEC-Cys) by the PEC method. Lin et al. (2007) demonstrated that the nanoparticles sized 110nm to 250nm composed of chitosan and poly(glutamic acid) loaded with 15% insulin were prepared with ionic gelation method. Despite numerous studies, the oral bioavailability of insulin is quite low and normally insufficient to have the desired systemic effect (Bayat, 2008). Therefore, developing an effective oral delivery system for these compounds has drawn increasing attention.

In this study, insulin nanoparticles were prepared and optimized using modified ionic gelation method. We applied dimethyle ethyle chitosan cystein (DMEC-Cys) polymer for development of nanoparticles with this method for the first time. This thiolated polymer with inter and intra disulfide bonds can form disulfide bonds with mucus glycoprotein and help to insulin delivery. Characterization of optimized nanoparticles, in vitro release test, FTIR and FE-SEM and cytotoxicity were also investigated

2. Material and Methods

2.1. Materials

Human insulin was obtained from Exir Pharmaceutical Co. (Lorestan, Iran). Dialyzing tube with a molecular cut-off of 12 kDa (D0530) was obtained from Sigma (Sigma-Aldrich, SaintLouis, MO). Analytical grade Lichrosolve acetonitrile was purchased from Merck (Darmstadt, Germany). Sodium tripolyphosphate anhydrous (TPP), Phosphoric acid and acetic acid were purchased from Sigma Aldrich (USA), (3-(4,5-trihydroxybenzoic acid) and (dimethylthiazol-2-yl) -2,5- diphenyltetrazolium bromide) (MTT) were obtained from Sigma Co. Ltd. (USA), HEK293 cell line (human embryonic kidney cells) was from the American Type Culture Collection (ATCC, Rockville, MD, USA), Dimethyl ethyl chitosan cysteine (DMEC-Cys) were prepared from pharmaceutical college. All other materials were of analytical grade and were used as received. Deionized water was used throughout this study for preparing solutions.

2.2. Preparation of insulin nanoparticles

Insulin nanoparticles were prepared by ionic gelation according to a modified method of Calvo et al. (1997) and based on the ionic

gelation of chitosan with TPP anions. Dimethyl ethyl chitosan cysteine (DMEC-Cys) was used as thiolated polymer that synthesized in pharmaceutical college of Tehran university (Mortazavian et al., 2014). This polymer included of 155 ($\mu\text{mol/g}$) -SH bond and 150 ($\mu\text{mol/g}$)-S-S- bond. Its molecular weight was 481 kg/mol and its zeta potential 35 mV. Initially, known amounts of polymer were dissolved in deionized water to obtain final concentrations of 0.5mg/mL, 0.75 mg/mL and 1 mg/mL (Table 1) under stirring at room temperature. Final pH of polymer was 4.

Table 1. Variables in Box-Behnken design and optimization procedure.

Factors	Levels used, Actual (coded)		
	(-1)	(0)	(+1)
X ₁ = DMEC-Cys (mg/mL)	0.5	0.75	1
X ₂ = TPP (mg/mL)	0.5	0.75	1
X ₃ = Insulin (mg/mL)	0.2	0.4	0.6
Responses	Constraints		
Y ₁ = Particle size (nm)	Minimize (with important index= 4)		
Y ₂ = PdI	Minimize		
Y ₃ = Zeta potential (mV)	Maximize		
Y ₄ = Association efficiency (%)	Maximize		

Subsequently, different amounts of insulin were dissolved in deionized water with pH 2 (using HCl), according to the Box-Behnken design; then, they premixed with different concentrations of TPP solution in proportion of 1:4. In many other references studied, they didn't mix these two solutions and TPP solution was added to polymer after drug solution. The volume proportion of polymer to insulin/TPP solution was 3:1, and the concentrations were prepared according to Box-Behnken design (Table 2).

In ionic gelation method, high pH would result in insulin nanoparticle with large particle size (Nasti et al., 2009). It is supposed that at low pH, the compacted nanoparticles have been fabricated due to electrostatic interaction between polymer and insulin. Also, the experiment should be carried out at pH below 6 and out of air to avoid the oxidation of thiol group which occurs in neutral and alkaline environment in adjacent to air (Dorkoosh et al., 2002).

Therefore, an acidic pH (pH<6) is a prerequisite when working with this polymer (DMEC-Cys). Due to formation of disulfide bond in pH > 6, it is understood that an increase in disulfide bond would lead to increase in the size of nanoparticles (Mortazavian et al., 2014).

Nanoparticles were prepared by adding insulin/TPP solution drop-wise to polymer solution under gentle magnetic stirring in 700 rpm at room temperature. Before mixing together, both solutions were passed through a syringe filter (pore size 0.45 μm , Biomill) to remove residues of insoluble particles.

Colloidal suspension was stirred for 25 min. and then centrifuged (Sigma 3K30, Osterode, Germany) for 20 min. at 1478 g and 4°C. The supernatant was used for the measurement of free insulin by high performance liquid chromatography (HPLC; SDV 505, Anyang, South Korea). Nanoparticles were re-suspended in demineralized water and freeze dried for next experiments.

In preparing of nanoparticles, the most important factors were selected on the basis of last researches and some parameters considered constant in all of experiments. Three factors of stirring rate (700 rpm), stirring time (25 min) and pH of polymer were

constant throughout the study and on the basis of the results of [Fàbregas et al., 2013](#)).
previous studies ([Vaezifar et al., 2013](#); [Mortazavian et al., 2014](#);

Table 2. Association efficiency (%), zeta potential, PDI and particle size of nanoparticles prepared in formulations of Box-Behnken experimental design*.

Run No.	Independent variables (Factors)			Dependent variables (Responses)			
	DMEC-cys (mg/mL)	TPP (mg/mL)	Insulin (mg/mL)	Size (nm)	PdI	Zeta potential (mv)	AE (%)
1	0.75	1	0.6	295.2±10.03	0.305±0.002	12.18±1.25	83.61±2.03
2	0.75	0.75	0.4	122±4.05	0.232±0.001	7.3±2.21	92.22±4.12
3	0.75	1	0.2	343±2.002	0.405±0.0112	7.1±6.25	83.31±3.11
4	0.75	0.5	0.2	183.0±1.04	0.253±0.0124	14.2±1.02	94.02±1.2
5	0.75	0.75	0.4	141.3±0.89	0.245±0.014	8.2±2.32	93.04±2.32
6	0.75	0.5	0.6	290.7±10.02	0.426±0.018	8.7±1.99	88.28±3.02
7	1	1	0.4	265.2±9.05	0.483±0.047	11±1.65	85.66±1.01
8	0.5	0.75	0.2	210.8±6.04	0.308±0.013	7.5±2.05	86.30±0.88
9	1	0.5	0.4	178.4±2.06	0.33±0.052	18.8±0.89	99.33±3.15
10	0.75	0.75	0.4	133.2±3.14	0.205±0.083	6.8±11.07	95.31±2.01
11	1	0.75	0.2	245.5±8.24	0.387±0.002	10.3±3.01	95.08±2.06
12	0.5	1	0.4	215.3±9.34	0.228±0.004	15±2.01	83.06±5.2
13	0.5	0.75	0.6	205.2±12.31	0.223±0.008	6.43±1.07	84.14±2.01
14	0.75	0.75	0.4	110.6±6.16	0.201±0.004	7.5±6.33	91.20±1.22
15	0.75	0.75	0.4	117.3±1.95	0.192±0.014	6.36±3.34	93.33±2.005
16	1	0.75	0.6	262.7±7.01	0.442±0.013	9.1±5.06	92.04±2.6
17	0.5	0.5	0.4	133.3±5.032	0.304±0.066	13.4±1.02	82.08±1.05

*Data are means ± SD (n = 3).

Table 3. Analysis of variance showing linear, quadratic and interaction variables and prediction model coefficients for characterizations of insulin nanoparticles.

Responses Source	df	Size		PdI		Zeta potential		AE (%)	
		Coefficient	p-value	Coefficient	p-value	Coefficient	p-value	Coefficient	p-value
Model	9	124.88	<0.0001	0.215	< 0.0001	7.232	< 0.0001	92.8	< 0.0001
X1	1	23.4	0.0006	0.072375	< 0.0001	0.85875	0.0268	4.5	< 0.0001
X2	1	41.66	<0.0001	0.0135	0.1380	-1.2275	0.0052	-3.625	< 0.0001
X3	1	8.93	0.0615	0.005375	0.5264	-0.33625	0.3102	-1.375	0.0158
X1X2	1	1.2	0.8387	0.05725	0.0015	-2.35	0.0010	-3.75	0.0005
X1X3	1	5.7	0.3489	0.035	0.0181	-0.0325	0.9425	-0.25	0.6960
X2X3	1	-38.87	0.0002	-0.06825	0.0006	2.645	0.0005	1.5	0.0445
X1 ²	1	13.12	0.0496	0.057	0.0014	2.55275	0.0005	-1.65	0.0282
X2 ²	1	60.05	<0.0001	0.06425	0.0007	4.76525	< 0.0001	-3.9	0.0003
X3 ²	1	93.05	<0.0001	0.068	0.0005	-1.45225	0.0110	-1.9	0.0156
Lack of fit	3		0.6255		0.4535		0.2230		0.8479
R ²			0.99		0.97		0.974		0.976

AE (%): Association Efficiency (%).

p-value < 0.05 is significant at $\alpha = 0.05$.

Lack of fit is not significant at p-value > 0.05.

2.3. Nanoparticle morphology

The morphology of nanoparticles was visualized by Field Emission Scanning Electron Microscopy (FE-SEM Hitachi, S4160, Tokyo, Japan). The nanoparticles were sputter-coated with gold for 10 min. at 6MA and 6kV (DC) under argon gas; and observed for morphology at an acceleration voltage of 20kV. Particle size diameter was determined using CLEMEX® particle image analysis software package.

2.4. Association efficiency of the Nanoparticles

An indirect method was used for determination of insulin encapsulation ([Avadi et al., 2010](#)). In this way, AE% was determined by subtracting the total amount of insulin used for

preparation of particles and the amount of non-encapsulated insulin present in the supernatant, according to equation 1.

$$AE\% = \frac{\text{Total amount of insulin} - \text{Free insulin in supernatant}}{\text{Total amount of insulin}} \times 100 \quad (1)$$

After centrifuging nanoparticles at 1478 g for 20 min., the supernatant was collected for determination of non-encapsulated insulin by HPLC; as reported previously ([Dorkoosh et al., 2002](#)). Fifty microliters of each sample were injected to Agilent10@ 1260 infinity equipped with 1260 ALS auto sampler, 1260 Quat pump VL and 1260 DAD VL detector that was set at 214 nm. The column used for chromatography was MZ® analytical PerfectSil Target (150*4.6 mm, 5 μ m).

Run time and flow rate were 10 min. and 0.5 mL/min, respectively. Mobile phase was consisted of 30% acetonitrile and 70% buffer containing 0.1 M KH₂PO₄ and 1% triethylamine adjusted to pH 2.8 with phosphoric acid. The data were obtained using Agilent ChemStation software.

2.5. Fourier transform infra-red spectroscopy (FTIR)

Nanoparticles separated from nanoparticulate suspensions were dried by a freeze dryer; and their FTIR transmission spectra obtained using FTIR (Perkin-Elmer Spectrum RX₁ System, Buckinghamshire, England) in the 400–4000 cm⁻¹ region, at room temperature and for changes in the intensity of sample peaks. However, FTIR was used to compare structural integrity of insulin in the presence and absence of nanoparticles. Fourier Transform Infrared Spectra (FTIR) of polymer (DMEC-Cys), TPP, insulin, nanoparticles and insulin loaded nanoparticles were recorded and compared together.

2.6. In vitro release study

In vitro release study was performed on the optimum nanoparticles and compared in two different pH phosphate buffer solutions (PBS) with pH 6.8 and 7.4, using dialysis method (Peng et al., 2012).

Dialysis bags with molecular weights cut off 12 KDa were used to allow the released insulin to permeate into the release medium. After adding freeze dried nanoparticles in PBS suspension into bag and tight bundling, the sample of loaded dialysis bag was soaked in 10 mL of PBS tube. The tube was placed on an oscillating water bath and incubated at 37±0.5°C with 100 strokes per min. 1 mL of release medium was collected and replaced with an equal volume of release medium reheated at 37°C to maintain sink conditions at predetermined time intervals for 4 h. The amount of insulin was determined by HPLC, as described previously (Manivasagan et al., 2013; Avadi et al., 2010).

2.7. Experimental Design

Systematic optimization procedures are carried out by selecting an objective function, finding the most important or contributing factors and investigating the relationship between responses and factors through the so called response surface methodology (Paul et al., 2015; Chopra et al., 2006; Motwani et al., 2008).

Design-Expert (version 8.0.7.1; Stat-Ease, Inc., Minneapolis, Minnesota, USA) software was used for mathematical modeling and assessment of the responses. The aim of optimization was to maximize the percentage of association efficiency and zeta potential while minimizing the particle size and PdI.

A Box–Behnken statistical design was used to evaluate and optimize the main effects, interaction effects and quadratic effects of independent variables on dependent variables. In this design, 3 factors in 3 levels were used to explore quadratic response surfaces and construct second-order polynomial models. This design was characterized by a set of points lying at the midpoint of each edge of a multidimensional cube and a center point replicate. The nonlinear computer-generated quadratic model was given as:

$$Y = S + AX_1 + BX_2 + CX_3 + ABX_1X_2 + BCX_2X_3 + ACX_1X_3 + A^2(X_1)^2 + B^2(X_2)^2 + C^2(X_3)^2 \quad (2)$$

Equation (2) was used to fit the experimental data of response variables for construction of the RSM model (Chopra et al., 2006; Wong et al., 1999). Where polymer (X₁), TPP (X₂) and the amount of insulin in the formulation (X₃) are the actual values of independent variables. Y is the corresponding response variable, S the constant; A, B and C are the linear coefficients; AB, BC and AC the interactive coefficients; and A², B² and C² are the quadratic coefficients. Subsequently, the maximum response variable and the corresponding variables were estimated from equation.

2.8. Data analysis, optimization and model validation

The responses and corresponding factors are modeled and optimized with Analysis of Variance (ANOVA) using a commercial statistical software package, Design-Expert 8.0.7.1 (Stat-Ease, Inc., Minneapolis, USA). The optimum formulation was determined using the Response Surface Methodology (RSM), which is a collection of mathematical and statistical techniques useful for modeling and analyzing problems (Wong et al., 1999).

The concentration range of independent variables under study along with their low, medium and high levels were selected base on the results from preliminary experimentation and using the results of other researcher (Table 1). According to Box–Behnken statistical design, 17 runs were examined. In this design, 12 factorial points with 5 replicates at the center point for calculation of pure error sum of squares were studied.

The significance of variables was determined by ANOVA through p-value less than 0.05. Also, no significant lack of fit (p-value > 0.05) is favorable because it indicates that the suggested model is properly, according to data obtained from different runs. To determine graphically the relationship and interactions between independent variables and responses, three dimensional surface plots were used in this study. Also, linear regression plots between actual and predicted values of the responses were produced.

3. Results and Discussion

3.1. Nanoparticle size

The uptake of polymer nanoparticles seems to be related to their size and superficial charge. The higher the superficial charge is, the stronger the affinity of the nanoparticles is for the negatively charged cell membrane. Nanoparticles with sizes ranging from 110.6 to 295.2 nm were obtained using different Box–Behnken runs. The results showed that Nanoparticles with the minimum particle size were achieved at run No. 14 and those with the maximum particle size fits to run No. 1 (Table 2). It is concluded from ANOVA results (Table 3) and was shown in three dimensional response surface plots (Fig. 1a) that, the concentrations of polymer solution (X₁) and TPP (X₂) have the most influence on the size of nanoparticles (p-value = 0.0006) and (p-value = 0.0001), respectively. As can be observed in this figure, mean diameter of particle size was increased with increasing the concentrations of polymer solution and TPP. Quadratic model was the best fitted model for particle size. Lack of fit was not significant (p-value=0.6255). Hence, these results indicated that equation 3 can be fitted properly on the data.

$$Y_1(\text{size}) = 124.88 + 23.4 (X_1) + 41.66 (X_2) + 8.93 (X_3) - 38.87 (X_2 X_3) + 13.12 (X_1)^2 + 60.05 (X_2)^2 + 93.05 (X_3)^2 \quad (3)$$

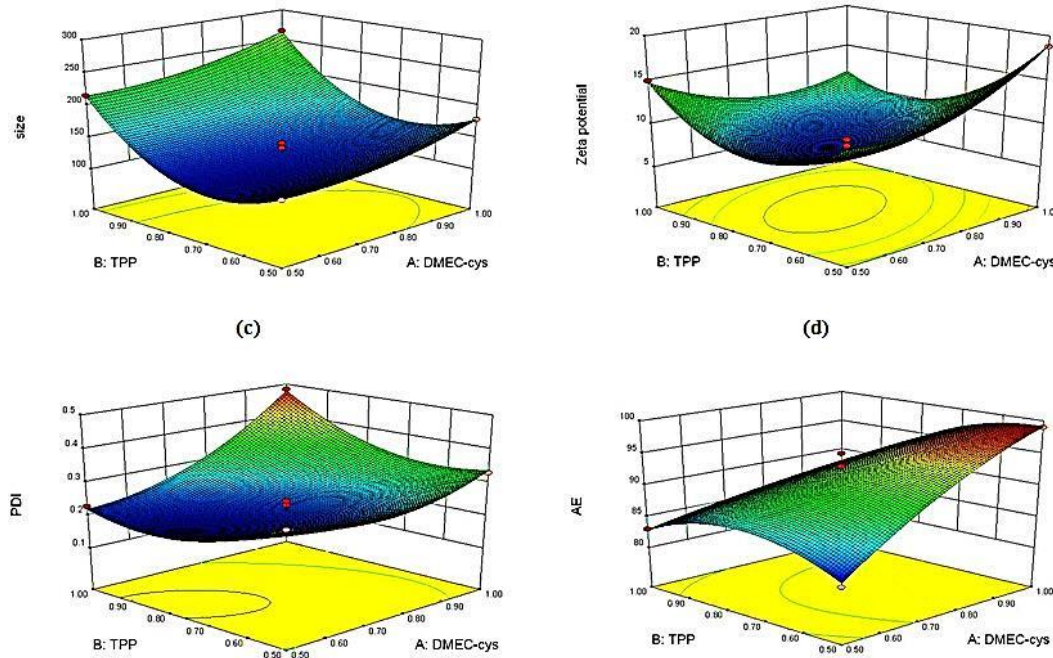


Fig. 1. 3-D response surface plots for a) size, b) zeta potential, c) PDI and d) AE% of insulin nanoparticles composed of DMEC-Cys polymer.

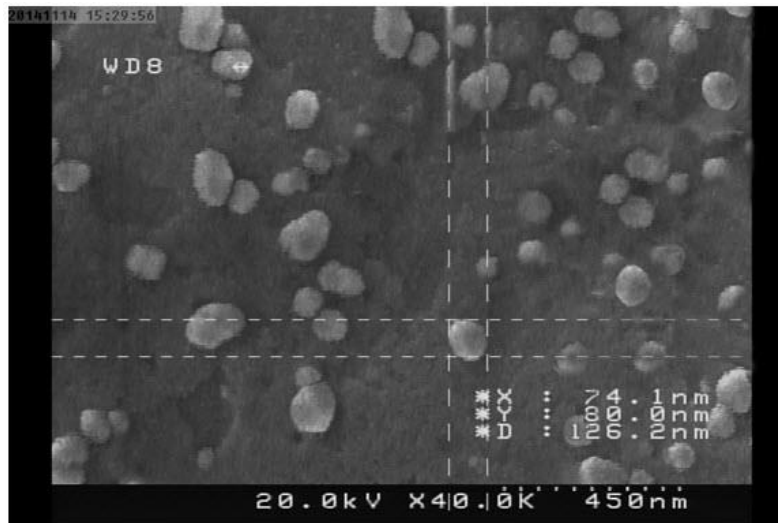


Fig. 2. SEM images of insulin loaded nanoparticles.

Dong et al. (2006) showed that increasing of chitosan concentration from 0.25 to 1 mg/mL caused size increasing from 152 nm to 232 nm. In other studies, the characteristics of chitosan/TPP particles prepared with different concentrations of chitosan or TPP were studied. The results indicated that the particle size increased with increasing the concentration of either chitosan or TPP (Fan et al., 2007; Vaezifar et al., 2013). In these concentration ranges, it seemed that the concentration of chitosan

or TPP has little effect on the mono dispersity of the nanoparticles; since their PDI values were all below 0.05 (Fan et al., 2007).

Researchers found that the formation of chitosan/TPP nanoparticles was only possible for some specific concentrations of chitosan and TPP (Calvo et al., 1997). This fact was also verified in our study that in order to avoid the formation of any microparticle, the concentration of chitosan or TPP needed to be below 1 mg/mL.

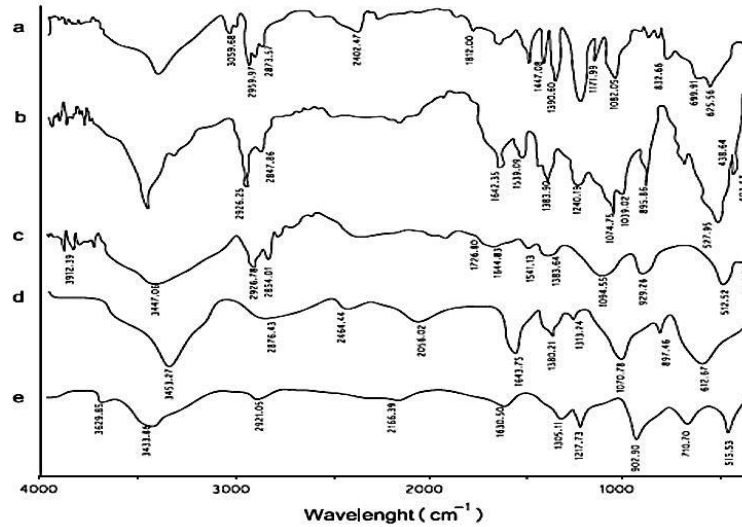


Fig. 3. FTIR spectra of (a) insulin (b) Insulin loaded nanoparticles (c) Nanoparticles (d) DMEC-Cys polymer (e) TPP.

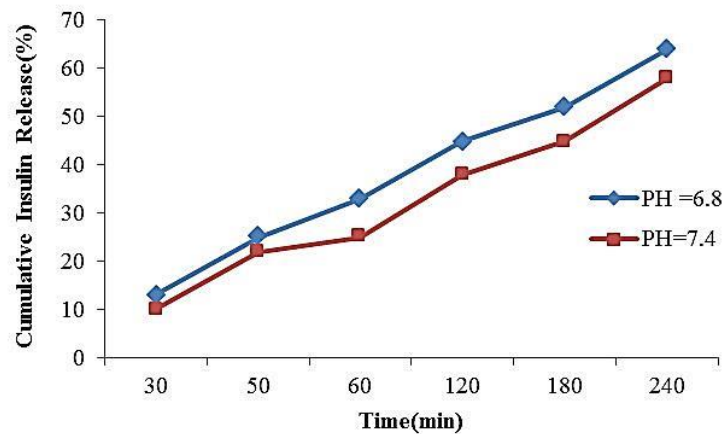


Fig. 4. In vitro release profiles of insulin from nanoparticles in PBS pH 6.8 and pH 7.4. Data presented as mean ± SD (n =2).

3.2. Zeta Potential

Zeta potential also is an important factor for the stability of nanosuspension. Stability of nanoparticles can be ensured by electrostatic repulsion force between particles. In other words, the stability of nanosuspension can be guaranteed when zeta potential rises. Particles with surface charge more than 30 mV may show cytotoxicity on the epithelial cells (Mortazavian et al., 2014). Nanoparticles with a positive surface charge are necessary for drug delivery (Lin et al., 2007; Sadeghi et al., 2008). As reported in the literature, there is a tendency to increase the zeta potential of nanoparticles with the increment of the chitosan concentration, which is attributed to the increase of NH³⁺ protonated groups of chitosan (Sadeghi et al., 2008; Woitiski et al., 2009).

Zeta potential of nanoparticles changed from 6.36 mV at run No.15 to 18.8 mV at run No. 9 (Table 2). It is concluded from ANOVA results and was also shown in 3-D plot (Fig. 1b) that, the concentrations of polymer (p-value=0.0268) and TPP (p-

value=0.0052) have the influence on zeta potential. This can be attributed to an increase in the total mass of positively charged polymer which leads to an increase in zeta potential of nanoparticles, which is due to availability of positively charged amino groups (Woitiski et al., 2009). Quadratic model was the best fitted model for zeta potential. Also, lack of fit was not significant (p-value=0.223). So, Equation 4 can be used to accurately predict the zeta potential of particles.

$$Y_3 (\text{zeta potential}) = 7.23 + 0.86(X_1) - 1.23(X_2) - 0.34(X_3) - 2.35(X_1X_2) - 0.033(X_1X_3) + 2.65(X_2X_3) + 2.55(X_1)^2 + 4.77(X_2)^2 - 1.45(X_3)^2 \quad (4)$$

As it is found in this study, all of the nanoparticles show positive charges. It is clear that positively charged particles are absorbed more than the neutral or negatively charged ones.

3.3. Polydispersity index

Polydispersity index (PdI), an expression of the homogeneity of nanosuspension, is ranged from 0 to 1. Where PdI tends to zero, the homogeneity of nanosuspension becomes higher than when PdI is equal to 1. PdI was fluctuating between minimum 0.192 at run No.15 and maximum 0.483 at run No.7 (Table 2). It is obvious from ANOVA (Table 3) that polymer concentration had the most significant factor that affected PdI (p-value=0.0001). As shown in Fig. 1c increasing the polymer concentration leads to an increase in PdI. Quadratic model was the best fitted model for PdI. Lack of fit was not significant (p-value=0.4535). Thus, equation 5 can be used to predict PdI.

$$Y_3 (\text{PdI}) = 0.22 + 0.072 (X_1) + 0.014 (X_2) + 5.37 * 10^{-3} (X_3) + 0.057 (X_1X_2) + 0.035 (X_1X_3) - 0.068 (X_2X_3) + 0.057(X_1)^2 + 0.064 (X_2)^2 + 0.068 (X_3)^2 \quad (5)$$

However, researchers showed that ionic gelation of nanoparticles had acceptable effect on particle size, zeta potential, PdI, encapsulation efficiency and the release of insulin which are in agreement with our findings. Furthermore, smaller particle and lower PdI have been accomplished by ionic gelation method (Yin et al., 2009).

3.4. Association Efficiency

A major advantage of ionic gelation method is that drug loading can be achieved without the aid of organic solvents or other harmful treatments. By this technique, more than 80% encapsulation efficiency was achieved with DMEC- Cys. According to results, the lowest AE was 82% at run No. 17 and the highest AE was 99% at run No. 9. ANOVA results showed that the concentration of polymer and TPP have the most important influence on AE% (p-value=0.0001). Concentration of insulin also was effective on AE% (P-value =0.0158).

Quadratic model was the best fitted model established for AE% by statistical analysis of experimental data; this is clearly shown with three-dimensional model graph for AE% in Fig. 1d. As it can be seen in this figure, by increasing the concentration of polymer, AE% was raised until the maximum level obtained. A research showed that flutamide drug entrapment increased by increasing the concentration of polymer in solution (Adlin et al., 2009). Lack of fit was not significant (p-value=0.8479). Therefore, equation 6 can be used to predict AE%.

$$Y_4 (\text{AE}\%) = 92.80 + 4.50(X_1) - 3.62(X_2) - 1.38(X_3) - 3.75(X_1X_2) - 0.25(X_1X_3) + 1.50(X_2X_3) - 1.65(X_1)^2 - 3.90(X_2)^2 - 1.90(X_3)^2 \quad (6)$$

3.5. Morphology of nanoparticles

In general, in vitro behaviour of nanoparticles tends to be greatly dominated by their physicochemical properties such as particle size, surface charge and shape of particles (Bayat et al., 2008). The morphology of insulin loaded nanoparticles was shown in Fig. 2. As it can be seen, particles look round to oval shape and no aggregation has been occurred. FE-SEM image showed that the size of droplets is almost equal to actual size measured by zetasizer.

3.6. Fourier transform infra-red spectroscopy (FTIR)

Nanoparticles separated from nanoparticulate suspensions were dried by a freeze dryer; and their FTIR transmission spectra obtained using FTIR (Perkin-Elmer Spectrum RX1 System, Buckinghamshire, England) in the 400–4000 cm^{-1} region, at room temperature and for changes in the intensity of sample peaks. However, FTIR was used to compare structural integrity of insulin in the presence and absence of nanoparticles.

The five Fourier Transform Infrared Spectra (FTIR) for nanoparticles, insulin loaded nanoparticles, DMEC-Cys, insulin and TPP were recorded on a Perkin Elmer FTIR spectrometer using KBr pellets to evaluate the cross linking of polymer with TPP and observe insulin structure before and after its loading into nanoparticles. They were mixed with KBr in the ratio of 1:10 and ground in a mortar by hand with a pestle. The powder was pressed into pellets under a pressure of 4t. The IR absorbency scans were analyzed between 400 to 4000 cm^{-1} for changes in the intensity of sample peaks (Fig. 3).

The figures exhibited the amide I, II and III bands; which are characteristics of proteins' IR spectra. Amide I band (~1650 cm^{-1}) corresponds mainly to the stretching vibration of the peptidic carbonyl group with a minor contribution from the out of phase C–N stretching vibration (Castrignanò et al., 2012). This band consists of a group of overlapped signals, which contains information on the secondary structure of the enzyme. The bands centered around 1545 cm^{-1} are assignable to the amide II band, which is due to the out of phase combination of the peptidic N–H in plane bend and the C–N stretching vibration. Additionally, the peak at 1517 cm^{-1} can be assigned to the C–C stretch and C–H bend of tyrosine side chain residues (Castrignanò et al., 2012). Moreover, a set of bands can be distinguished in the region about 1200 and 1300 cm^{-1} . It can be assigned to the amide III mode, associated to the in phase combination of the peptidic N–H with C–N bending vibration.

However, comparison of the spectra recorded for insulin in the presence or absence of NPs showed no significant differences in the secondary structure, confirming that the interaction of insulin with NPs does not compromise the structural integrity of this protein (Castrignanò et al., 2012; Sarmiento et al., 2006). In another study, no significant differences were found when comparing the secondary structure composition of insulin in the absence or presence of nanoparticles. Moreover, these results are in agreement with previously published results on the protein secondary structure (Castrignanò et al., 2012).

Fig. 3(a-b) shows the FTIR spectrum of insulin loaded nanoparticles and without nanoparticles. It is well known that the peaks at 2926 and 1383 cm^{-1} are mainly associated with polymer that became obvious in nanoparticles. These spectra are attributed to HC=C asymmetrical stretching and N=O bond, respectively. The intensity of these spectra increased in insulin loaded nanoparticle, because of conjugation of insulin molecules on surface or interior of nanoparticles.

In Fig. 3a, Nps spectrum in 3000-3750 cm^{-1} are due to the stretching vibrational frequency of N-H groups on Nps surface. The spectra of 3386, 1074 and 1240 cm^{-1} were attributed to hydrogen bonded O-H stretch, C-O stretch and C-O stretch, respectively. Also 2854, 2847 and 1726 cm^{-1} spectra are attributed to C-H stretch. C-H stretch, C=O stretch and the peaks of 1644 and 1642 are related to C=O or C=C stretch. 1541 and 1539 cm^{-1} spectra were because of N-H bend that increased its intensity for insulin nanoparticle; and spectra of 895, 929, 527 and 512 cm^{-1} were attributed to C-H bonds.

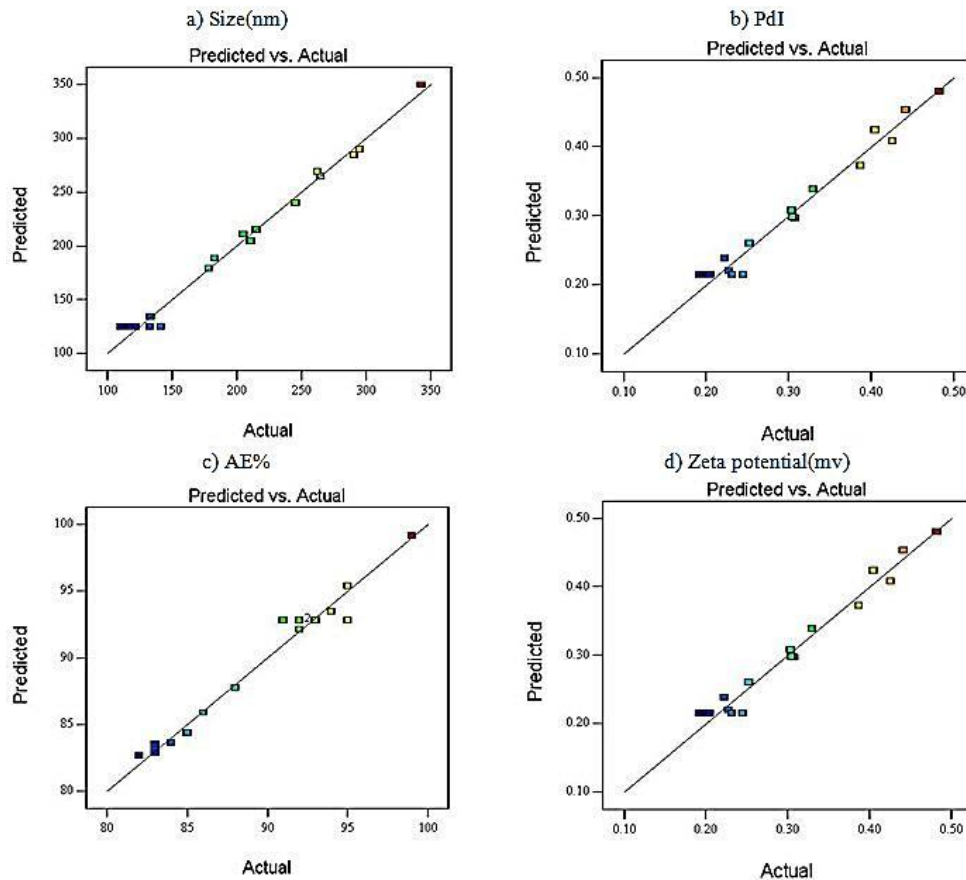


Fig. 5. Linear correlation plots (a, b, c, d) between actual and predicted values for different responses.

As shown in Fig. 3a, some specific bands in insulin disappeared due to special peaks of insulin overlapping after they were loaded into the nanoparticles.

Fig. 3c shows the FTIR of pure insulin, which has characteristic peaks at 3331, 3059, 2959, 1812, 1447, and 699 cm^{-1} . The TPP spectrum in Fig. 3e shows multiple characteristic peaks at 3392, 2921, 1217, 902, 754 and 570 cm^{-1} . Also, FTIR of insulin showed 333, 2959, 2873 and 1666 cm^{-1} spectra; because of C-OH, C-H, C-H and C=C bonds.

The pure polymer chemical groups were assessed using FTIR spectroscopy. Its spectrum (Fig. 3d) shows the peaks around 897 and 1154 cm^{-1} because of the saccharide structure, the peaks at 1643 and 1313 cm^{-1} because of amides I and III, and the sharp peaks at 1371 and 1431 cm^{-1} because of the CH symmetrical deformation. The peaks at 1070 and 1039 cm^{-1} because of the C-O stretching vibration and a broad peak at 3453 cm^{-1} because of the amine N-H symmetrical vibration are also shown. The spectrums about 3453, 2876, 1070, 612 and 1643 cm^{-1} were because of C-OH, C-H, C-O stretch and C-H bonds. These results also indicated that TPP, DMEC-Cys polymer and insulin had good mutual integration.

3.7. In vitro release study

Insulin release was studied as a function of time. The in vitro release profiles from optimized DMEC-Cys nanoparticles compared in pH 6.8 and pH 7.4 is illustrated in Fig. 4. The release

rate from nanoparticles in PBS of pH 6.8 was found to be approximately similar to pH 7.4. As it can be seen in this figure, insulin released from DMEC-Cys nanoparticles after 30 min. in pH 6.8 and pH 7.4 were 13.2 and 11.42 %, respectively. These results demonstrate that these nanoparticulate systems have a small burst release and indicate appropriate interaction between insulin and polymer. According to Fig. 4, the cumulative release of insulin at pH 6.8 and pH 7.4 in nanoparticles composed of DMEC-Cys and within 240 min. were 64.32 %, and 58.72%, respectively.

These results show that this system has a small burst effect and then sustained release characteristics for 4h, indicating a good insulin encapsulation. However, loading drugs by ionic gelation method has a relatively small burst release and sustained release characteristics due to the additional cross linking of the polymer with TPP that possesses a denser matrix structure and hence a lesser availability of the incorporated insulin at the beginning of release experiments (Sadeghi et al., 2008). The drug could be associated to the nanoparticles in three different states: (a) at the nanoparticle surface, (b) in the core as a reversible complex with polymer, or (c) in the core as an irreversible complex with polymer. The repartition of the peptide between these three states depends on the initial peptide concentration. Size and repartition of the peptide inside nanoparticles influence the release rate (Sadeghi et al., 2008).

This study showed the little faster release profile of insulin at pH 6.8 than pH 7.4 for nanoparticles composed of DMEC-Cys and can be justified by considering the fact that this polymer possesses the high solubility in neutral aqueous media. In another study,

release profile were compared for fabricated nanoparticles with two methods of PEC and IG; and the release of insulin was slower from nanoparticles made according to ionotropic gelation method (Sadeghi et al., 2008). Our results showed that these systems have a small burst effect and then sustained-release characteristics for 4 hours, indicating a good insulin encapsulation in nanoparticles; also, there are no significant differences in release profile of nanoparticles in PBS, pH 6.8 and 7.4.

3.8. Optimization and model validation

The optimum nanoparticle formulation was obtained by Box-Behnken design based on the constraints of physicochemical parameters for insulin nanoparticles. The optimum condition was at concentration 0.89 mg/mL of DMEC-Cys, 0.52 mg/mL of TPP and 0.33 mg/mL of insulin. Physicochemical characterization of optimized nanoparticles was 148 nm, 15.5 mV, 0.26 and 97.56% for particle size, zeta potential, PdI and AE, respectively.

The validity of Box-Behnken design for the optimization of insulin nanoparticle formulation is demonstrated by predicted error which is lower than 5%. For validation of the model, experiments were carried out by using the optimum conditions as described above. Percentage prediction error helped in evaluating the validity of generated regression equations. Prediction error for four response variables was found to vary between -2/88% and +2/52%. Linear correlation plots between the actual and the predicted response variables (Fig. 5) showed the scatter of the residuals versus actual values for better representation of the spread of dependent variables under present experimental settings.

4. Conclusion

Abstract In this study, one thiolated quaternary ammonium of chitosan (DMEC-Cys) was used for fabricating insulin nanoparticles by IG method. The effect of different variables on nanoparticle preparation was investigated. The results have indicated a small size, positive charge and good AE for nanoparticles. The technique, an extremely mild and simple process, yielded nanoparticles with reproducible size (110 to 295 nm) and encapsulation efficiency of 83% to 99%. Nanoparticles were optimized by response surface method. The most important factors affecting the responses were identified and the relationship between the factors was investigated. Using Box-Behnken design leads to optimized nanoparticles with minimum particle size, PdI, maximum zeta potential and entrapment efficiency. Morphological study revealed the spherical formation of nanoparticle without aggregation. The results of in vitro release of this study revealed suitable interaction between DMEC-Cys conjugate and insulin. Also, they indicated that nanoparticles prepared by quaternized derivatives of chitosan seem to be a promising vehicle for oral administration of proteins and peptides. However, more studies, such as ex vivo and in vivo studies, are necessary to fully evaluate the potential of this nanoparticulate system as a delivery platform for oral peptides and proteins delivery and absorption.

References

Adlin, J., Gowthamarajan, K., & Somashekhara, C. (2009). Formulation and evaluation of nanoparticles containing flutamide. *International journal of ChemTech research*, 1(4), 1331-1334.

- Avadi, M. R., Sadeghi, A. M. M., Mohammadpour, N., Abedin, S., Atyabi, F., Dinarvand, R., & Rafiee-Tehrani, M. (2010). Preparation and characterization of insulin nanoparticles using chitosan and Arabic gum with ionic gelation method. *Nanomedicine: Nanotechnology, Biology and Medicine*, 6(1), 58-63.
- Bayat, A., Larijani, B., Ahmadian, S., Junginger, H. E., & Rafiee-Tehrani, M. (2008). Preparation and characterization of insulin nanoparticles using chitosan and its quaternized derivatives. *Nanomedicine: Nanotechnology, Biology and Medicine*, 4(2), 115-120.
- Calvo, P., Remunan-Lopez, C., Vila-Jato, J. L., & Alonso, M. J. (1997). Novel hydrophilic chitosan-polyethylene oxide nanoparticles as protein carriers. *Journal of Applied Polymer Science*, 63(1), 125-132.
- Calvo, P., Vila-Jato, J. L., & Alonso, M. J. (1997). Evaluation of cationic polymer-coated nanocapsules as ocular drug carriers. *International Journal of Pharmaceutics*, 153(1), 41-50.
- Castrignanò, S., Sadeghi, S. J., & Gilardi, G. (2012). Entrapment of human flavin-containing monooxygenase 3 in the presence of gold nanoparticles: TEM, FTIR and electrocatalysis. *Biochimica et Biophysica Acta (BBA)-General Subjects*, 1820(12), 2072-2078.
- Chopra, S., Patil, G. V., & Motwani, S. K. (2006). Response surface methodology for optimization of losartan potassium controlled release tablets. *Journal of Controlled Release*, 2(116), e102-e104.
- Couvreur, P. (2013). Nanoparticles in drug delivery: past, present and future. *Advanced drug delivery reviews*, 65(1), 21-23.
- Dong, Y., Ng, W. K., Shen, S., Kim, S., & Tan, R. B. (2013). Scalable ionic gelation synthesis of chitosan nanoparticles for drug delivery in static mixers. *Carbohydrate polymers*, 94(2), 940-945.
- Dorkoosh, F. A., Verhoef, J. C., Ambagts, M. H., Rafiee-Tehrani, M., Borchard, G., & Junginger, H. E. (2002). Peroral delivery systems based on superporous hydrogel polymers: release characteristics for the peptide drugs busserelin, octreotide and insulin. *European journal of pharmaceutical sciences*, 15(5), 433-439.
- Fàbregas, A., Miñarro, M., García-Montoya, E., Pérez-Lozano, P., Carrillo, C., Sarrate, R., ... & Suñé-Negre, J. M. (2013). Impact of physical parameters on particle size and reaction yield when using the ionic gelation method to obtain cationic polymeric chitosan-tripolyphosphate nanoparticles. *International journal of pharmaceutics*, 446(1-2), 199-204.
- Fan, W., Yan, W., Xu, Z., & Ni, H. (2012). Formation mechanism of monodisperse, low molecular weight chitosan nanoparticles by ionic gelation technique. *Colloids and Surfaces B: Biointerfaces*, 90, 21-27.
- Hu, B., Pan, C., Sun, Y., Hou, Z., Ye, H., Hu, B., & Zeng, X. (2008). Optimization of fabrication parameters to produce chitosan-tripolyphosphate nanoparticles for delivery of tea catechins. *Journal of Agricultural and Food Chemistry*, 56(16), 7451-7458.
- Jamshidi, L. (2012). Educational needs of diabetic patients whom referred to the diabetes center. *Procedia-Social and Behavioral Sciences*, 31, 450-453.
- Khafagy, E. S., Morishita, M., Onuki, Y., & Takayama, K. (2007). Current challenges in non-invasive insulin delivery systems: a comparative review. *Advanced drug delivery reviews*, 59(15), 1521-1546.
- Lin, Y. H., Mi, F. L., Chen, C. T., Chang, W. C., Peng, S. F., Liang, H. F., & Sung, H. W. (2007). Preparation and characterization of nanoparticles shelled with chitosan for oral insulin delivery. *Biomacromolecules*, 8(1), 146-152.
- Manivasagan, P., Venkatesan, J., Senthilkumar, K., Sivakumar, K., & Kim, S. K. (2013). Biosynthesis, antimicrobial and cytotoxic effect of silver nanoparticles using a novel *Nocardiosis* sp. MBRC-1. *BioMed research international*, 2013.
- Mohammadpouroungh, N., Behfar, A., Ezabadi, A., Zolfagharian, H., & Heydari, M. (2010). Preparation of chitosan nanoparticles containing *Naja naja oxiana* snake venom. *Nanomedicine: Nanotechnology, Biology and Medicine*, 6(1), 137-143.
- Morishita, M., Goto, T., Nakamura, K., Lowman, A. M., Takayama, K., & Peppas, N. A. (2006). Novel oral insulin delivery systems based on complexation polymer hydrogels: single and multiple administration studies in type 1 and 2 diabetic rats. *Journal of Controlled Release*, 110(3), 587-594.

- Mortazavian, E., Amini, M., Dorkoosh, F. A., Amini, H., Khoshayand, M. R., Amini, T., & Rafiee-Tehrani, M. (2014). Preparation, design for optimization and in vitro evaluation of insulin nanoparticles integrating thiolated chitosan derivatives. *Journal of Drug Delivery Science and Technology*, 24(1), 40-49.
- Motwani, S. K., Chopra, S., Talegaonkar, S., Kohli, K., Ahmad, F. J., & Khar, R. K. (2008). Chitosan-sodium alginate nanoparticles as submicroscopic reservoirs for ocular delivery: Formulation, optimisation and in vitro characterisation. *European Journal of Pharmaceutics and Biopharmaceutics*, 68(3), 513-525.
- Nagavarma, B. V. N., Yadav, H. K., Ayaz, A. V. L. S., Vasudha, L. S., & Shivakumar, H. G. (2012). Different techniques for preparation of polymeric nanoparticles-a review. *Asian journal of pharmaceutical and clinical research*, 5(3), 16-23.
- Nasti, A., Zaki, N. M., de Leonardis, P., Ungphaiboon, S., Sansongsak, P., Rimoli, M. G., & Tirelli, N. (2009). Chitosan/TPP and chitosan/TPP-hyaluronic acid nanoparticles: systematic optimisation of the preparative process and preliminary biological evaluation. *Pharmaceutical research*, 26(8), 1918-1930.
- Paul, S., Jayan, A., & Sasikumar, C. S. (2015). Physical, chemical and biological studies of gelatin/chitosan based transdermal films with embedded silver nanoparticles. *Asian Pacific Journal of Tropical Disease*, 5(12), 975-986.
- Peng, Q., Zhang, Z. R., Gong, T., Chen, G. Q., & Sun, X. (2012). A rapid-acting, long-acting insulin formulation based on a phospholipid complex loaded PHBHHx nanoparticles. *Biomaterials*, 33(5), 1583-1588.
- Sadeghi, A. M. M., Dorkoosh, F. A., Avadi, M. R., Saadat, P., Rafiee-Tehrani, M., & Junginger, H. E. (2008). Preparation, characterization and antibacterial activities of chitosan, N-trimethyl chitosan (TMC) and N-diethylmethyl chitosan (DEMC) nanoparticles loaded with insulin using both the ionotropic gelation and polyelectrolyte complexation methods. *International Journal of Pharmaceutics*, 355(1-2), 299-306.